Limnol. Oceanogr., 48(3), 2003, 1150–1160

Measurements of phosphate affinity constants and phosphorus release rates from the microbial food web in Villefranche Bay, northwestern Mediterranean

Tsuneo Tanaka[1] *and Fereidoun Rassoulzadegan*
LOV-UMR7093, Station Zoologique, BP 28, F-06234 Villefranche-sur-Mer, France

T. Frede Thingstad
University of Bergen, Department of Microbiology, Jahnebakken 5, P.O. Box 7800, N-5020 Bergen, Norway

Abstract

Using ^{32}P, uptake and transfer of phosphorus in the microbial food web were studied in surface water from Villefranche Bay (northwestern Mediterranean) from September to December 2001. During the study, the thermocline gradually declined and vertical mixing started, leading to a transition from a nutrient-depleted period to a nutrient-replete period. Before vertical mixing started, the orthophosphate turnover time ranged from 1 to 5 h. Orthophosphate uptake was dominated by the 0.6–2 μm size fraction (mean, 70%), where the cyanobacteria biomass was dominant. The estimated affinity constants for bacteria, cyanobacteria, and autotrophic nanoflagellates ranged from 0.001 to 0.028, 0.047 to 0.103, and 0.002 to 0.032 L nmol P^{-1} h^{-1} during the period, with relatively short (<5 h) orthophosphate turnover times. These results suggest that cyanobacteria were superior for orthophosphate uptake among osmotrophs. For cyanobacteria and autotrophic nanoflagellates, the mean affinity constants were almost at the theoretical maximum predicted by diffusion-limited uptake. On the basis of a cold-chase technique, release rates of dissolved ^{32}P from labeled particles were $<0.5\%$ h^{-1}, which corresponds to a turnover time of the particulate fraction up to three orders of magnitude greater than that of orthophosphate. Although a net loss of ^{32}P occurred in the 0.2–0.6 and 0.6–2 μm fractions, a net increase in the >2 μm fraction suggested P transfer to the larger size fraction by predation. Viruses did not contribute significantly to ^{32}P release from bacteria during the study period.

Inorganic nutrients (e.g., N and P) are used by osmotrophs—for example, heterotrophic bacteria and phytoplankton—in aquatic systems. Previous studies in the Mediterranean Sea have revealed high nitrate : phosphate ratios compared with the Redfield ratio (N : P = 16) (Krom et al. 1991), a response to phosphate addition in the growth rate of bacteria (Zweifel et al. 1993; Thingstad et al. 1998; Zohary and Robarts 1998) and a turnover time of orthophosphate as short as 40 min during the stratified period (Thingstad et al. 1998). Such results suggest that Mediterranean surface water becomes P limited for bacteria and phytoplankton during stratified periods.

In an environment with a permanently low substrate concentration, it is the maximum specific affinity constant that determines the competitive ability between osmotrophs (Vadstein 2000). The theoretical maximum value for the affinity constant is given by diffusion limitation—that is, when all substrate molecules diffusing toward the cell are captured. For spherical cells with similar internal concentrations of the limiting element, this maximum specific affinity decreases with the inverse square of cell radius (Jumars et al. 1993); the theory thus predicts that heterotrophic bacteria should be superior competitors to phytoplankton for P uptake because of the difference in cell size. This has led to the argument of the bacteria-phytoplankton paradox: ''why do not P-limited bacteria outcompete phytoplankton until phytoplankton biomass is reduced to a level where bacteria become carbon-limited'' (Bratbak and Thingstad 1985)? However, this paradox can be resolved by taking into account predators that control the biomass of the winning competitor (Pengerud et al. 1987; Thingstad and Lignell 1997). Therefore, to understand the mechanisms that control material cycling and flux in P-deficient systems, it is essential to understand not only the competitive relationship between bacteria and phytoplankton but also the predator-prey interactions of bacteria and phytoplankton—that is, the microbial food web.

In autumn in Villefranche Bay (northwestern Mediterranean), Dolan et al. (1995) found that orthophosphate uptake was always dominated by the 0.2–1 μm fraction. Coinciding with the erosion of the thermocline, PO_4 uptake within the >1 μm size fraction shifted toward organisms sized >10 μm. Using a cold chase, these authors estimated slow rates ($\leq 1\%$ h^{-1}) of phosphorus release from the particulate fraction. However the 0.2–1 μm fraction evidently included ''heterotrophic and autotrophic'' bacteria (Dolan et al. 1995), which prevented a clear distinction between heterotrophic bacteria and phytoplankton in PO_4 uptake. Because cyanobacteria can be dominant in primary production and bacterial production can be nearly 50% of primary production in surface water in Villefranche Bay (Hagström et al. 1988), it is

[1] Present address: University of Bergen, Department of Microbiology, Jahnebakken 5, PO Box 7800, N-5020 Bergen, Norway (tsuneo.tanaka@im.uib.no).

Acknowledgments

We thank D. Betti and J.-Y. Carval for field sampling; E. J. Rochelle-Newall for preparing virus concentrates; C. Gache, G. Lhomond, and J. Croce for use of the facilities at the isotope laboratory. The data for water temperature and Chl *a* were given by the Service d'Observation en Milieu Littoral. T.T. was partly supported by Bergen Marine Food Chain Research Infrastructure. This study was supported by the EC through project CYCLOPS (EVK3-CT-1999-00009).

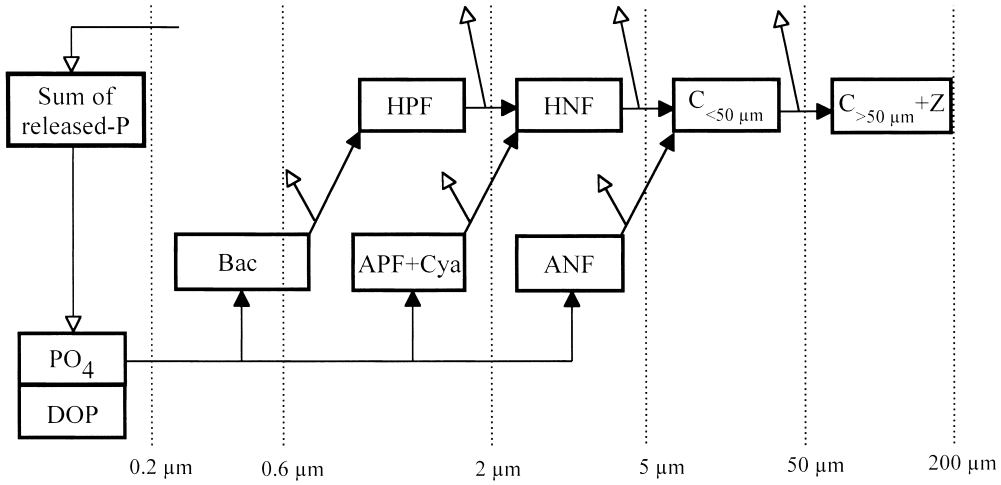

Fig. 1. Flow structure of the model used for estimating P stock, flux, and turnover time of each compartment. Phosphorus enters a simplified microbial food web through absorption and ingestion (black arrows) and is released by predators (white arrows). The model consists of PO_4 (bioavailable free orthophosphate), DOP, Bac (heterotrophic bacteria), APF + Cya (autotrophic picoflagellates and cyanobacteria), ANFs, HPFs, HNFs, $C_{<50\mu m}$ (ciliates <50 μm), and $C_{>50\mu m}$ + Z (ciliates >50 μm, tintinnids, and mesozooplankton). Large phytoplankton (e.g., diatoms) were not considered. The size fractions are shown at the bottom of the flow diagram. See text for details.

crucial to get separate estimates of the affinity constant for heterotrophic bacteria and cyanobacteria.

Our objective was to estimate the affinity constants of bacteria, autotrophic picophytoplankton (dominantly cyanobacteria), and autotrophic nanoflagellates (ANFs) for orthophosphate. We also measured the fluxes of phosphorus in whole or size-fractionated microbial communities during the season with relatively short orthophosphate turnover times. Then the essential aspects of microbial phosphorus cycling in Villefranche Bay in autumn was explored by combining the measured P biomass and fluxes with a simple model based on bacteria-phytoplankton competition for P and P transfer by protozoan predation on osmotrophs (Fig. 1; Thingstad et al. 1997, 1999).

Materials and methods

Sampling—Sampling was conducted at Point B in Villefranche Bay in the northwestern Mediterranean (43°41′10″N, 7°19′00″E; 80 m maximum depth) from September to December 2001. Water samples were collected at 10 m using a Niskin bottle and were transported to the laboratory within 30 min, where they were prescreened through 200-μm nylon mesh to remove large zooplankton.

Phosphorus measurements—Soluble reactive phosphorus (SRP), total dissolved phosphorus (TDP), and particulate phosphorus were measured spectrophotometrically using the molybdenum blue reaction described by Koroleff (1976). SRP was measured in triplicate without filtration. TDP was measured in triplicate after an acid persulphate oxidation, at 121°C, of 0.2-μm filtrates. The detection limit was ~0.03 μmol L^{-1} for both SRP and TDP. Dissolved organic phosphorus (DOP) was calculated by subtracting SRP from TDP. As for particulate P, 500-ml samples were filtered sequentially through 47-mm polycarbonate filters with 2, 0.6, and 0.2 μm pore sizes. Filters were transferred to polypropylene test tubes with 15 ml of Milli-Q water and then treated as TDP samples. No replicates were done for particulate P samples.

Size fractionation of bacteria and algae—To separate bacteria, cyanobacteria, and ANFs into different size fractions, we examined the portion of each group that passed through filters with different pore sizes. Samples from Point B were filtered through polycarbonate filters with 2- and 1-μm pore sizes by gravity and with 0.6-μm pore size under low-vacuum pressure (<0.07 bar). Samples for cell counts were prepared from filtrates as mentioned later.

Uptake of $^{32}PO_4^-$—Uptake kinetics of orthophosphate was measured according to the method of Thingstad et al. (1993). Carrier-free ^{32}P orthophosphate (ICN Biomedicals) was added to 10-ml samples in 20-ml polyethylene vials to give a final radioactive concentration ~10^5–10^6 counts per minute (CPM) ml^{-1}. Samples for subtraction of background and abiotic adsorption were fixed with 100% trichloroacetic acid before isotope addition. Samples were incubated at in situ temperature (±2°C) and subdued (laboratory) illumination for an incubation time that varied between 15 min and 2 h, according to the expected turnover time. Incubation was stopped by a cold chase of 100 mmol L^{-1} KH_2PO_4 (final concentration, 1 mmol L^{-1}). Aliquots were filtered in parallel on 25-mm polycarbonate filters with 2, 0.6, and 0.2 μm pore sizes, respectively. All filters were placed on a Millipore 12-place manifold and supported on Whatman GF/C filters saturated with 100 mmol L^{-1} KH_2PO_4. To alleviate the need for rinsing and to obtain low blanks (Suttle et al. 1990), the vacuum was kept low during filtration through the 2- and 0.6-μm filters, increased to 0.2 bar during filtration through

0.2-μm filters, and finally increased to >0.6 bar to remove any water remaining on the filters. This filtration process was always completed within 30 min after the cold-chase addition. Filters were placed in polyethylene scintillation vials with Milli-Q water and radioassayed with a Beckman LS 1800 scintillation counter.

The kinetics of orthophosphate uptake were determined by the Rigler bioassay (1966). Unlabelled KH_2PO_4 was added to 10-ml samples (0, 25, 50, 75, and 100 nmol L^{-1}, respectively) prior to isotope addition. The incubation was stopped after 15 min by the addition of cold KH_2PO_4 and uptake of ^{32}P was measured, as mentioned above. All counting results were transformed into the fraction of particulate ^{32}P to total ^{32}P per hour. Turnover time, maximum uptake rates (V_{max}), and the sum $K_{PO_4} + S_n$ (the half-saturation constant and the natural concentration of bioavailable orthophosphate, respectively) were calculated according to the method of Wright and Hobbie (1966) as modified by Thingstad et al. (1993).

Calculation of affinity constants—Specific affinity constants were estimated according to the procedure proposed by Thingstad and Rassoulzadegan (1999) as follows. Under the assumption that the uptake in heterotrophic bacteria is proportional to the substrate concentration (S_n) and biomass (B_B), one has $\alpha_B S_n B_B = f_B V$, where α_B is the specific affinity and f_B is the fraction of total uptake (V) that goes into heterotrophic bacteria. Because the turnover time $T = S_n/V$, solving for α_B gives $\alpha_B = (f_B/T)/B_B$. Correspondingly, for α_P (the specific affinity of picophytoplankton) and α_N (ANFs), $\alpha_P = (f_P/T)/B_P$ and $\alpha_N = (f_N/T)/B_N$, where B_P and B_N are the biomass of autotrophic picoflagellates (APFs) plus cyanobacteria and ANFs, respectively.

Under the assumption that the 0.2–0.6 μm fraction contains a fraction (b) of total heterotrophic bacteria and that all bacteria are equally active, $f_B = f_{0.2\text{–}0.6\mu m}/b$, so that

$$\alpha_B = [(f_{0.2\text{–}0.6\mu m}/b)/T]/B_B$$

Uptake in the 0.6–2 μm fraction contains both a bacterial part $(1 - b)f_B V$ and an uptake by APFs and cyanobacteria $f_P V$, so that $f_{0.6\text{–}2\mu m} = (1 - b)f_B + f_P$. Solving for f_P, this gives $f_P = f_{0.6\text{–}2\mu m} - [(1 - b)/b]f_{0.2\text{–}0.6\mu m}$. Thus,

$$\alpha_P = (\{f_{0.6\text{–}2\mu m} - [(1 - b)/b]f_{0.2\text{–}0.6\mu m}\}/T)/B_P$$

Under the assumption that the uptake in the >2-μm fraction is only by ANFs ($f_N = f_{>2\mu m}$), the similar reasoning gives

$$\alpha_N = (f_{>2\mu m}/T)/B_N$$

P transfer experiments—On three occasions (10 and 25 October and 8 November), cold-chase experiments were performed, to study the effect of food web structure on ^{32}P transfer between different size fractions. This was done on water prefiltered through polycarbonate filters with 0.6, 2, and 5 μm pore sizes and nylon filters with 50 and 200 μm mesh sizes, to remove different sized predators, and on the <0.6 μm filtrates enhanced with virus concentrate. Virus-concentrated water was prepared by prefiltration through GF/F and 0.2-μm filters, followed by concentration that used a 100-kDa filter cartridge attached to a tangential flow ultrafiltration system (Millipore Prep/Scale TTF system with a polyethersulphone Prep/Scale cartridge). SRP and TDP in the concentrated water were measured in triplicate. Virus concentrate was added into <0.6 μm filtrate to give 10 times the nominal enhancement of viruses. We refer to this treatment as the <0.6 μm + V filtrate. Each filtrate (200 ml) was incubated in three 250-ml polycarbonate bottles for measuring net growth rates of microbial components and in one bottle for measuring ^{32}P transfer rates (see below). For the <200 μm filtrate, an extra bottle was served as the control (see below). Incubation was done at in situ temperature (±2°C) and subdued (laboratory) illumination for 48 h. For net growth rate estimates, samples for microscopic counts were taken in triplicate at the start and the end of incubation.

Carrier-free ^{32}P orthophosphate was added to 200-ml filtrates that passed through different filter pore sizes. To prevent the reassimilation of recycled orthophosphate, all filtrates but one of two <200-μm filtrates were given a cold chase of 100 mmol L^{-1} KH_2PO_4 (final concentration, 100 or 200 μmol L^{-1}) at 3 h after isotope addition. During the incubation, 10-ml samples were periodically taken and filtered on 2, 0.6, and 0.2 μm filters for counting particulate ^{32}P. In addition, 5-ml samples were taken and filtered through 0.2 μm DynaGard hollow-fiber syringe filters. Filtrates were transferred into polyethylene vials for dissolved ^{32}P measurement.

P flow diagram in the food web—If one assumes a food-web structure for P flow and combines this with the assumption of an approximate steady state, the data collected in P transfer experiments can be used to give a rough estimate of P fluxes between microbial components in the Villefranche Bay ecosystem (Fig. 1). The calculations are analogous to those used by Thingstad et al. (1993) for analyzing P transfer in the microbial food web of a Norwegian fjord.

In brief, by using the microscope-based estimates of heterotrophic bacterial biomass P (nmol P L^{-1}) and combining this with the specific release rate of ^{32}P (h^{-1}) from the 0.2–0.6 μm fraction as obtained from the cold-chase experiments (<200 μm filtrates), an absolute loss rate (nmol P L^{-1} h^{-1}) from heterotrophic bacteria can be calculated after correction for the portion that heterotrophic bacteria were retained on the 0.6 μm filter (*see* ''Results'' section). Under the assumption that P loss is balanced by uptake of orthophosphate, this calculation also gives a bacterial uptake rate that, once combined with measured fraction of ^{32}P uptake, allows the computation of absolute uptake rates (nmol P L^{-1} h^{-1}) into the 0.6–2 and >2 μm size fractions. Multiplying an estimate of the total uptake rate by a turnover time of orthophosphate gives the concentration of bioavailable free orthophosphate. If the nonliving particulate P is assumed to be negligible, the subtraction of microscope-based biomass P of ANFs, heterotrophic nanoflagellates (HNFs), and ciliates <50 μm ($C_{<50\mu m}$) from the chemically measured particulate P (2–200 μm) gives the biomass P of larger predators (50–200 μm) that consist of ciliates >50 μm, tintinnids, and mesozooplankton ($C_{>50\mu m}$ + Z).

Under the assumption that only negligible amounts of ^{32}P were transferred from the osmotrophs to their phagotroph predators during the 3-h pre–cold-chase phase, one can es-

Table 1. Monthly means (±SD) of temperature (°C), Chl *a* (μg L^{-1}), and microbial abundance (cells L^{-1}) at 10 m of Point B from September to December 2001.

	Sep	Oct	Nov	Dec
Temperature	19.4 ± 2.6	21.4 ± 1.0	18.0 ± 1.3	15.9 ± 0.9
Chl *a*	0.39 ± 0.38	0.14 ± 0.05	0.15 ± 0.05	0.15 ± 0.02
	(n = 3)	(n = 5)	(n = 4)	(n = 4)
Bacterial ($\times 10^8$)	6.7 ± 0.7	6.9 ± 1.2	6.3 ± 1.9	4.8
Cyanobacteria ($\times 10^7$)	3.7 ± 0.4	3.7 ± 1.0	2.0 ± 0.9	1.3
HPF ($\times 10^5$)	<0.07	0.8 ± 0.5	1.2 ± 0.6	0.8
APF ($\times 10^5$)	0.5 ± 0.2	1.1 ± 1.0	1.5 ± 1.1	3.1
HNF ($\times 10^5$)	1.4 ± 0.5	3.8 ± 1.6	4.9 ± 1.4	3.6
ANF ($\times 10^5$)	2.7 ± 0.9	6.3 ± 2.8	8.8 ± 2.1	4.8
	(n = 3)	(n = 7)	(n = 5)	(n = 1)
Oligotrich ciliates	nd	2,200 ± 756	1,440 ± 57	80
Tintinnids	nd	100 ± 72	90 ± 42	60
	(n = 0)	(n = 3)	(n = 2)	(n = 1)

n, number of data, nd = no data. Data on temperature and Chl *a* are from SOMLIT (2002).

timate the efficiency of P transfer from prey to predator after the cold chase. Multiplying the radioactivity at 3 h in each size fraction (CPM ml^{-1}) by the respective specific release rate of ^{32}P (h^{-1}) estimated during the post–cold-chase phase gives gross loss rates of ^{32}P for bacteria, APFs + cyanobacteria, and ANFs, respectively (CPM ml^{-1} h^{-1}). The sum of ^{32}P loss rates in three size fractions can be considered the total gross loss rate. Comparing this with the appearance rate of dissolved ^{32}P (i.e., net loss rate) in the <200 μm filtrates with cold chase gives an efficiency of P transfer from prey to predator: transfer efficiency = (gross loss rate − net loss rate)/(gross loss rate). If this efficiency is assumed to be the same in all predator-prey transfers, the flow diagram can be completed. Under the assumption that the remaining output from the highest predator level ($C_{>50\mu m}$ + Z) in our model is returned to the dissolved pool, the diagram is closed, with P release to dissolved pool balancing P uptake to osmotrophs.

Abundance of microbial components—Samples for microscopic counts were fixed with glutaraldehyde (final concentration, 1%) for picoplankton and nanoplankton and with acid Lugol's (final concentration, 2%) for ciliates. Heterotrophic bacteria, cyanobacteria, picoflagellates (<2 μm), and nanoflagellates (2–10 μm) were counted by epifluorescence microscope after staining with 4′6-diamidino-2-phenylindole (DAPI) (Porter and Feig 1980). Oligotrich ciliates and tintinnids were counted by inverted microscope after sedimentation on Utermöhl chamber.

To estimate the biomass P of microbial components, we chose the following conversion factors: 20 fg C $cell^{-1}$ for bacteria (Lee and Fuhrman 1987), 200 fg C $cell^{-1}$ for cyanobacteria, 183 fg C μm^{-3} for flagellates (Caron et al. 1995), 0.19 pg C μm^{-3} for oligotrich ciliates (Putt and Stoecker 1989), and 0.053 pg C μm^{-3} for tintinnids (Verity and Langdon 1984). With regard to flagellates and ciliates, we assumed a constant volume for each size class: 4.2 μm^3 $cell^{-1}$ for <2 μm, 35 μm^3 $cell^{-1}$ for 2–5 μm, and 294 μm^3 $cell^{-1}$ for 5–10 μm for flagellates, and 4×10^3 μm^3 $cell^{-1}$ for <30 μm, 2.15×10^4 μm^3 $cell^{-1}$ for 30–50 μm, and 4.7×10^4 μm^3 $cell^{-1}$ for >50 μm for ciliates. We used a C : P ratio of 50 for bacteria (Fagerbakke et al. 1996) and 106 for the other groups (Redfield et al. 1963).

Regression analysis—Linear regression analysis was used to calculate the changing rates of ^{32}P and cell abundance in each size fraction. The former was calculated as the slope of relative concentration (percentage of added radioactivity) versus time (h) for the period from the cold-chase addition to the end of incubation or for the period of linear portion. The latter was calculated as the slope of the natural log of plankton abundance (cells L^{-1}) versus time (h). The statistical significance was tested for each regression and for the regression slope comparisons between different size fractions or groups (Student's *t*-test; Sokal and Rohlf 1995).

Results

Environmental variables and microbial abundance—The thermocline deepened from September toward mid-November, when the stratification of the water column broke down (Service d'Observation en Milieu Littoral 2002). Chlorophyll *a* concentrations at 10 m were usually <0.2 μg L^{-1}, except at the beginning of September (Table 1; Service d'Observation en Milieu Littoral 2002).

The TDP concentration ranged from 0.28 to 0.51 μmol L^{-1}, except for two very high values on 10 October and 30 November (Fig. 2A). SRP values varied from below the limit of detection to 0.07 μmol L^{-1} (Fig. 2B) but were always <20% of TDP. Particulate P varied from 0.008 to 0.05 μmol L^{-1} (Fig. 2B). Except on 25 September, the fraction of particulate P was 35%–72% (mean, 50%) for >2 μm, 19%–52% (mean, 30%) for 0.6–2 μm, and 10%–33% (mean, 20%) for 0.2–0.6 μm (Fig. 2C).

Bacteria, cyanobacteria, oligotrich ciliates, and tintinnids were less variable during the study period, whereas HNFs and ANFs increased from September to October and then remained stable until December (Table 1). Temporal variations in abundance of heterotrophic picoflagellates (HPFs) and APFs were similar to those of nanoflagellates.

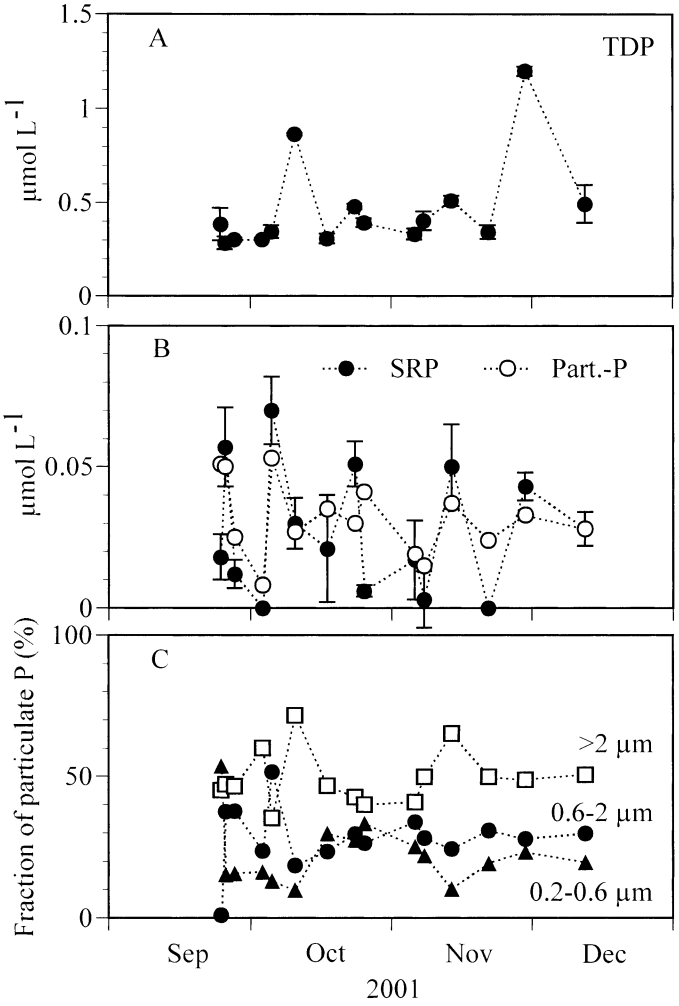

Fig. 2. Temporal variations in concentration of (A) TDP, (B) SRP and particulate P (μmol L^{-1}), and (C) fraction of particulate P (%) at 10 m, Point B, Bay of Villefranche from September to December 2001. TDP and SRP are mean ± SD (n = 3).

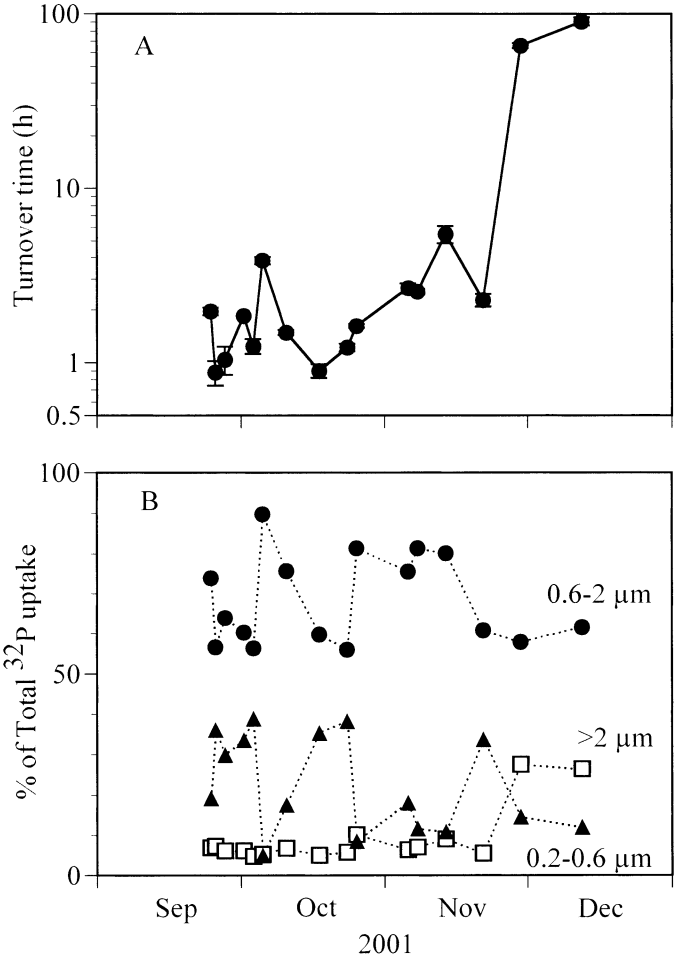

Fig. 3. Same as Fig. 2 but (A) ^{32}P orthophosphate turnover time (h) (mean ± SD, n = 3) and (B) fraction of ^{32}P uptake (%).

P uptake kinetics—Orthophosphate turnover time ranged from 0.9 to 90.7 h (Fig. 3A). From September to October, it usually fluctuated between 1 and 2 h and then increased slightly to 2.5–5 h in November. From mid-November to December, it increased greatly, to 90.7 h.

From September to mid-November, $^{32}PO_4$ uptake was dominated by the 0.6–2 μm fraction (56.0%–89.8%; mean, 69.4%), followed by the 0.2–0.6 μm fraction (4.9%–38.9%; mean, 24.0%) and the >2 μm fraction (4.7%–10.2%; mean, 6.6%) (Fig. 3B). Coinciding with the increase of turnover time in December, the >2 μm fraction increased to ~30%.

The results of isotope dilution experiments were well described by a linear regression (r^2 = 0.805–0.998; Table 2). The estimated $K_{PO_4} + S_n$ in the 0.2–0.6 μm fraction was lower than that in the two larger size fractions. The estimated V_{max} was always greatest in the 0.6–2 μm fraction.

Microscopic examination revealed that almost all bacteria and pico-sized autotrophic phytoplankton (cyanobacteria and APFs) passed through the 2-μm-pore filters and that the <0.6 μm filtrates included ~75% of bacteria and very few cyanobacteria (Table 3). Therefore, we assumed that the >2 μm fraction includes mainly ANFs, the 0.6–2 μm fraction included 25% of heterotrophic bacteria, all cyanobacteria, and APFs, and the 0.2–0.6 μm fraction included 75% of bacteria: we applied 75% to "*b*" for estimations of affinity constants. Because our procedure assumed that P uptake is approximated by a linear relationship—that is, the balanced substrate limited growth—we calculated affinity constants only for the period with a relatively short turnover time (<5 h, 25 September–22 November) (Fig. 4). The affinity constants in the 0.6–2 μm fraction were greater than those in the >2 and 0.2–0.6 μm fractions, ranging from 0.001 to 0.028 L nmol P^{-1} h^{-1} (mean, 0.011) for the 0.2–0.6 μm fraction (α_B), 0.047 to 0.103 L nmol P^{-1} h^{-1} (mean, 0.068) for the 0.6–2 μm fraction (α_P), and 0.002 to 0.032 L nmol P^{-1} h^{-1} (mean, 0.012) for the >2 μm fraction (α_N).

Effects of prefiltration on microbial groups and on P transfer in the food web—Table 4 shows microbial groups whose abundance changed significantly during incubation and a comparison of changing rates between different filtrates for each microbial group (Student's *t*-test; $P < 0.05$). On 10 October, ANFs significantly decreased in all three

Table 2. Turnover time for orthophosphate-^{32}P (mean ± SD, n = 3), its distribution between size fraction, and V_{max} and $K_{PO4} + S_n$ estimates.

Date	Turnover time (h)	% of uptake			V_{max} (nmol-P L^{-1} h^{-1})			$K_{PO4} + S_n$ (nmol-P L^{-1})			r^2		
		0.2–0.6 μm	0.6–2 μm	>2 μm	0.2–0.6 μm	0.6–2 μm	>2 μm	0.2–0.6 μm	0.6–2 μm	>2 μm	0.2–0.6 μm	0.6–2 μm	>2 μm
26 Sep 01	0.88 ± 0.14	0.36	0.57	0.07	3.17	15.44	2.77	16.99	18.11	41.32	0.925 (n = 5)	0.911 (n = 5)	0.805 (n = 3)
03 Oct 01	1.24 ± 0.12	0.39	0.56	0.05	0.35	11.55	0.92	4.74	40.26	43.74	0.993 (n = 3)	0.858 (n = 5)	0.869 (n = 4)
05 Oct 01	3.84 ± 0.20	0.05	0.90	0.05	nd	12.10	0.81	nd	47.85	56.91	nd	0.890 (n = 5)	0.998 (n = 3)
17 Oct 01	0.90 ± 0.08	0.35	0.60	0.05	0.58	14.51	2.17	4.60	23.44	56.16	0.958 (n = 3)	0.993 (n = 5)	0.869 (n = 4)

nd, no data.

filtrates (<5, 50, and 200 μm), among which the decrease rate was highest in the <50 μm filtrate. This suggests that ANFs were ingested mainly by predators of 5–50 μm. Bacteria showed net increases only in the <0.6 μm and <0.6 μm + V filtrates, which indicates top-down control on bacteria. Bacterial increase was greater in the <0.6 μm + V filtrate than in <0.6 μm. On 25 October, ANFs decreased only in the <200 μm filtrate. Cyanobacteria increased in three filtrates (<2, 5, and 200 μm), and the increase rate was greater in the <2 and <5 μm filtrates. This suggests that cyanobacteria and ANFs were ingested by predators of 5–200 μm. Bacteria increased significantly in all filtrates, and the highest increase rate was found in the 0.6 μm + V filtrate. On 8 November, HNFs and ANFs decreased in the <200 μm filtrate, which suggests a significant predation on nanoflagellates. Bacteria increased in all four filtrates, and the increase rate was lowest in the <200 μm filtrate. The main bacterivores appeared to be in the 5–200 μm fraction.

The time course of the percentage of added ^{32}P measured on 8 November is shown as an example (Fig. 5). After a cold chase, the percentage of added ^{32}P generally showed linear change until the end of incubation. The <200 μm filtrates without cold chase showed no significant net release of ^{32}P (<0.2 μm), except on 10 October ($P > 0.05$, Student's t-test) (Fig. 6). Multiplying the total particulate P concentration (0.2–200 μm) by the release rate of dissolved ^{32}P, the P release flux from the total microbial community was estimated to be 0.12, 0.16, and 0.06 nmol P L^{-1} h^{-1} on 10 and 25 October and 8 November, respectively.

On 10 October, a significant release of dissolved ^{32}P was observed subsequent to cold chase in all filtrates (Fig. 6A). The release rates were significantly greater in the <200, <50, and <5 μm filtrates (0.41%–0.50% of added ^{32}P h^{-1}) than in the <0.6 μm and <0.6 μm + V filtrates (0.23% of added ^{32}P h^{-1}). The increase of dissolved ^{32}P was accompanied by a significant net decrease of label in the 0.6–2 and 0.2–0.6 μm fractions (0.17%–0.30% of added ^{32}P h^{-1}), except in the 0.2–0.6 μm fraction of the <200 μm filtrate. However, the >2 μm fraction showed a significant increase in the <200 μm filtrate without cold chase and the <5 μm filtrate (0.07% and 0.04% of added ^{32}P h^{-1}).

On 25 October, a significant release of ^{32}P after cold chase was observed in the <200, <5, and <2 μm filtrates (0.40%–0.49% of added ^{32}P h^{-1}). However, a significant decrease was detected only in the 0.6–2 μm fraction (0.27%–0.35% of added ^{32}P h^{-1}) (Fig. 6B).

On 8 November, a significant release was observed in the <200 and <5 μm filtrates (0.44% and 0.36% of added ^{32}P h^{-1}), whereas no significant decrease was observed in the 0.2–0.6 and 0.6–2 μm fractions (Fig. 6C). A significant increase in the >2 μm fraction was found in the <200 and <5 μm filtrates (0.15% and 0.12% of added ^{32}P h^{-1}) as well

Table 3. Effects of filter pore sizes on size-fractionation of bacteria, cyanobacteria, and APFs. The data are shown as average % of total abundance.

Filtrates	Bacteria	Cyanobacteria	APF	n
<2 μm	94.2	102.2	103.3	3
<1 μm	91.2	79.2	96.7	3
<0.6 μm	76.5	0.8	≈0	9

n, number of data.

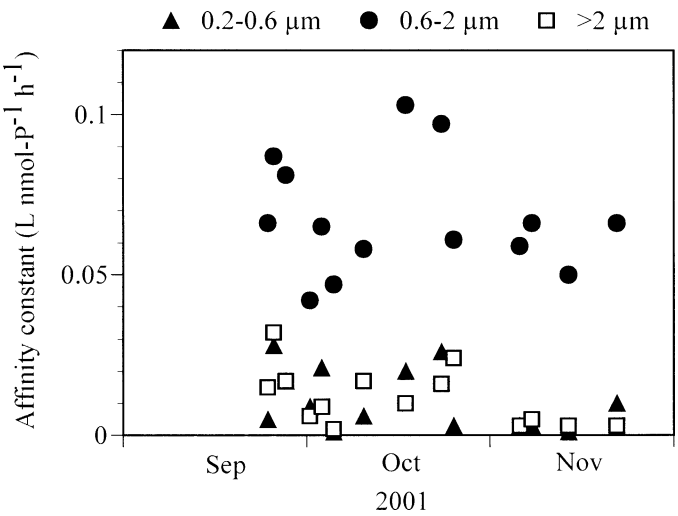

Fig. 4. The estimated affinity constants in the 0.2–0.6 (α_B), 0.6–2 (α_P), and >2 μm (α_N) fractions from 25 September to 22 November, when ^{32}P orthophosphate turnover time was relatively short (<5 h). See text for details.

Table 4. Regression analysis of time-course change of microbial abundance in different sizes of filtrates ($n = 6$ for all cases).

Date of experiment	Prepared filtrates	Group*	Rate (h^{-1})	95% confidence limits of rate	r^2	P	Difference between filtrates†
10 Oct 10	<200 μm	Cililates	−0.015	0.008	0.868	0.007	
		ANFs	−0.018	0.013	0.801	0.016	<50 μm
	<50 μm	Ciliates	−0.014	0.007	0.902	0.004	
		ANFs	−0.038	0.011	0.957	0.001	<5, 200 μm
		APFs	−0.039	0.024	0.838	0.010	
	<5 μm	ANFs	−0.021	0.014	0.799	0.016	<50 μm
	<0.6 μm	Bacteria	0.007	0.005	0.815	0.014	
	<0.6 μm + V	Bacteria	0.013	0.005	0.937	0.002	
25 Oct 01	<200 μm	Ciliates	−0.026	0.014	0.868	0.007	
		ANFs	−0.015	0.012	0.738	0.028	
		Cyanobacteria	0.006	0.002	0.937	0.002	<2, 5 μm
		Bacteria	0.005	0.001	0.991	<0.001	<0.6 μm + V
	<5 μm	Cyanobacteria	0.010	0.003	0.966	<0.001	<200 μm
		Bacteria	0.006	0.004	0.807	0.015	<0.6 μm + V
	<2 μm	Cyanobacteria	0.010	0.002	0.977	<0.001	<200 μm
		Bacteria	0.005	0.003	0.853	0.009	<0.6 μm + V
	<0.6 μm	Bacteria	0.009	0.009	0.693	0.040	
	<0.6 μm + V	Bacteria	0.012	0.004	0.940	0.001	<2, 5, 200 μm
08 Nov 01	<200 μm	Ciliates	−0.016	0.008	0.895	0.004	
		HNF	−0.008	0.008	0.679	0.044	
		ANF	−0.027	0.020	0.785	0.019	
		Bacteria	0.003	0.001	0.917	0.003	<0.6 μm + V, 0.6, 5 μm
	<5 μm	Bacteria	0.006	0.002	0.949	0.001	<200 μm
	<0.6 μm	Bacteria	0.008	0.003	0.936	0.002	<200 μm
	<0.6 μm + V	Bacteria	0.006	0.002	0.948	0.01	<200 μm

<0.6 μm + V = 0.6-μm filtrates with virus-enhanced water.
* Only the groups whose abundance changed significantly during the incubation (*t*-test, $P < 0.05$).
† Rate comparisons between filtrates were shown for each group (*t*-test, $P < 0.05$).

as in the <200 μm filtrate without cold chase (0.17% of added $^{32}P\ h^{-1}$). In the <0.6 μm + V filtrate, although no significant release was detected, ^{32}P in the 0.2–0.6 μm fraction decreased significantly.

P flow in the microbial food web—On the basis of the cold-chase experiments, stocks, rates of uptake and release, and turnover times in the P flow diagram (Fig. 1) are summarized in Table 5. The P biomass of the microbial components varied a factor of less than three between three dates, whereas P uptake into microbial components varied a factor of two to four. As a result, the turnover time of microbial biomass P varied up to a factor of eight. As shown in Fig. 3B, P flux into APFs + cyanobacteria dominated among osmotrophs, and the turnover time of this component was shortest and varied little. Among predators, the greatest P uptake and release were generated by HNFs, which are assumed to ingest APF + cyanobacteria in the diagram, and the second greatest by small ciliates ($C_{<50\mu m}$) that ingest HNFs.

The estimated concentration of bioavailable free orthophosphate ranged from 1.3 to 2.3 nmol L^{-1}, which were less than the detection limit in this study and were two orders of magnitude lower than DOP. The estimated P release rate ranged from 0.14 to 0.29 nmol P $L^{-1}\ h^{-1}$.

Discussion

In Villefranche Bay, the surface mixed layer is gradually cooled down, and the water column stratification breaks down from late summer to early winter. As a result, nutrients in the surface water change from depleted to replete. This leads to an increase of large-sized phytoplankton (Rassoulzadegan 1979) and a great increase in the orthophosphate turnover time (Dolan et al. 1995; this study). For a marine system, the turnover times of orthophosphate found in the present study were relatively short (<2 h) from September to October and were consistent with an assumed P deficiency for osmotrophs in surface water.

Affinity constants of heterotrophic bacteria, cyanobacteria, and ANFs—The estimated affinity constants of pico-sized phytoplankton dominated by cyanobacteria were greater than those of not only ANFs but also of heterotrophic bacteria. However, a similar unexpected conclusion has recently been reached from a Mediterranean study by Moutin et al. (2002). In a review of published data, Vadstein and Olsen (1989) reported affinity constants for orthophosphate in the range of 0.03–0.15 L nmol $P^{-1}\ h^{-1}$ for bacteria and 0.001–0.017 L nmol $P^{-1}\ h^{-1}$ for phytoplankton. Compared with these values, our estimates were lower for bacteria,

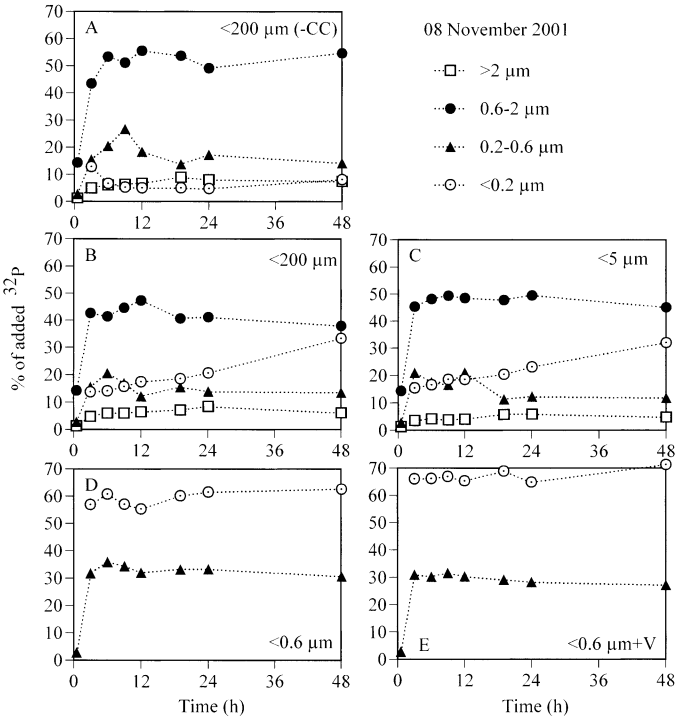

Fig. 5. Distribution of ^{32}P in the <0.2, 0.2–0.6, 0.6–2, and >2 μm fractions for (A) <200 μm (−CC, without cold chase), (B) <200 μm, (C) <5 μm, (D) <0.6 μm, and (E) <0.6 μm + V filtrates during the incubation on 8 November. A cold chase was added 3 h after the addition of ^{32}P except for the data labeled −CC.

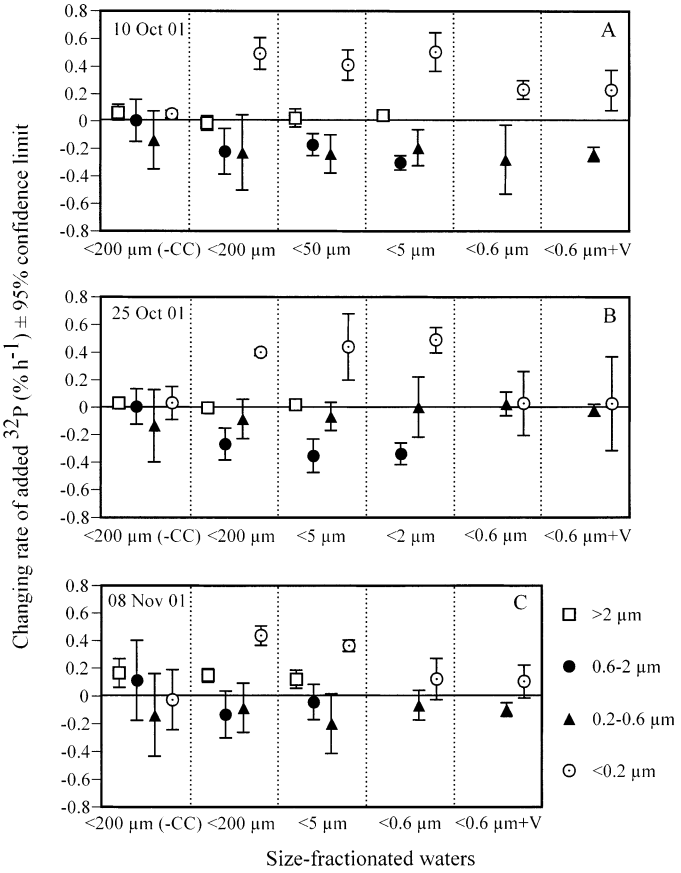

Fig. 6. Changing rates of added ^{32}P (±95% confidence limit) in the <0.2, 0.2–0.6, 0.6–2, and >2 μm fractions for different sizes of prefiltered water over incubation time on (A) 10 October, (B) 25 October, and (C) 8 November, respectively.

greater for cyanobacteria, and within the reported range for ANFs. However, because previous studies of affinity constants for P were based on different methods, it may be difficult to compare estimated values in detail. On the other hand, the comparison with studies that used a methodology similar to ours showed that the maximum affinity constant for cyanobacteria is slightly lower in the northwestern Mediterranean (0.103 L nmol P^{-1} h^{-1}, this study) than in the eastern Mediterranean (0.25 L nmol P^{-1} h^{-1}, Moutin et al. 2002), and the mean of our estimates for ANFs (0.012 L nmol P^{-1} h^{-1}) corresponds well to what was found for phytoplankton in the >1 μm fraction in Sandsfjord, Norway (0.013 L nmol P^{-1} h^{-1}, Thingstad et al. 1993).

The affinity constants estimated in the present study can be compared with those given by diffusion limitation of substrate transport to the cell surface—that is, the theoretical maximum (Fig. 7; *see also* Thingstad and Rassoulzadegan 1999):

$$\alpha = (3D/\sigma)/r^2$$

where D is the diffusion constant for the substrate molecules (assumed to be $\approx 10^{-5}$ cm^2 s^{-1}), σ is the internal concentration of P, and r is the cell radius of osmotrophs. σ is derived from the assumption that bacteria and phytoplankton cells have a density of 1.2 g cm^{-3}, 50% dry weight of wet weight, and 50% carbon of dry weight and that the C : P ratio is 50 for bacteria and 106 for phytoplankton. r is assumed to be 0.25, 1, and 2 μm for heterotrophic bacteria, cyanobacteria, and ANFs, respectively. The mean affinity constants for cyanobacteria and ANFs were fairly close to those predicted by the diffusion model. This indicates that cyanobacteria and ANFs were P deficient from September to November and that cyanobacteria were the winning competitor among osmotrophs in terms of PO_4 uptake.

The reason for the low affinity constants estimated for bacteria is unknown. One possibility, contradictory to the conclusion of Thingstad et al. (1998), could be that the growth rate of heterotrophic bacteria was limited by factors other than phosphate. Another possibility could be artifacts in our estimation procedure. The proposed procedure to estimate affinity constants requires the measurements of ^{32}P orthophosphate turnover time, the fraction of ^{32}P taken by each group, and the biomass P of each group or size fractionated particulate P (Thingstad and Rassoulzadegan 1999). The sources of artifact can be from incomplete separation of groups by size fractionation and errors in estimation of biomass P or size fractionated particulate P. Unless the small portion of bacteria retained in the 0.6–2 μm fraction was highly active in terms of PO_4 uptake, we believe that the effect of an imperfect size fractionation was minimized by our modified procedure.

Because the particulate P measurements include both living and nonliving particles with the incomplete fractionation, we used biomass P for affinity constant estimation. The bio-

Table 5. Stocks (nmol-P L^{-1}), rates of uptake and release (nmol-P L^{-1} h^{-1}), and turnover times (h) of each compartment in the P flow diagram (Fig. 1), estimated from the cold-chase experiments (*see text for explanation*).

Date	Parameter	PO_4		DOP	Bac	APFs + Cya	ANFs	HPFs	HNFs	$C_{<50\mu m}$	$C_{>50\mu m}$ + Z
10 Oct 01	Stock*	1.52		834	25	0.02, 8.1	2.1	0.05	2.5	4.3	10.4
	Uptake		0.29†		0.29	0.71	0.07	0.26	0.64, 0.24‡	0.06, 0.79§	0.77
	Turnover time	1.42		nd	86	11	31	0.2	3	5	13
	Release							0.03	0.07, 0.03‡	0.01, 0.08§	0.08
25 Oct 01	Stock*	2.32		384	27	0.01, 7.9	2.1	0.05	1.4	2.5	10.5
	Uptake		0.19†		0.11	1.22	0.15	0.11	1.16, 0.10‡	0.15, 1.21§	1.29
	Turnover time	1.57		nd	242	6	14	0.4	1.1	2	8
	Release							0.01	0.05, 0.005‡	0.01, 0.06§	0.06
08 Nov 01	Stock*	1.27		399	20	0.03, 4.6	4	0.07	2.3	2	nd
	Uptake		0.14†		0.11	0.38	0.04	0.10	0.34, 0.09‡	0.03, 0.39§	0.38
	Turnover time	2.43		nd	185	12	105	0.7	5.5	5	nd
	Release							0.01	0.04, 0.01‡	0.004, 0.04§	0.04

Bac, bacteria, Cya, cyanobacteria, nd, no data.
* DOP stocks are based on the chemically measured TDP and particulate P (Fig. 2). Microbial biomass-P is based on microscope counts and conversion factors (*see* Materials and methods section). P stock in APF + Cya shows the biomass P of APFs and Cya, respectively.
† The sum of P release from HPFs, HNFs, $C_{<50\mu m}$, and $C_{>50\mu m}$ + Z.
‡ P uptake or release from APFs + Cya and from HPFs into HNFs, respectively.
§ P uptake or release from ANFs and HNFs into $C_{<50\mu m}$, respectively.

mass P depends on abundance measurements of osmotrophs, conversion factors from cell abundance or volume to carbon, and C : P ratios. Although it is difficult to quantify *Prochlorococcus* by epifluorescence microscope (Chisholm et al. 1988), high-performance liquid chromatography analysis has revealed that they are not abundant in autumn at the study site (Bustillos-Guzmán et al. 1995), which suggests that the abundance of osmotrophs was not underestimated. The comparison of our estimates with the theoretical maximum suggests that this inherent problem was insignificant, at least for picophytoplankton and ANFs (Fig. 7). An overestimation of bacterial P or of the active fraction of this (here assumed to be 100%) would lead to α_B being underestimated. Recent studies have reported that only 2%–32% of total bacterium-sized particles were nucleoid-containing bacteria (Zweifel and Hagström 1995), 34% of free-living bacteria were intact (Heissenberger et al. 1996), and 3%–5% of total bacteria were cyanoditolyl tetrazolium chloride (CTC) positive or actively respiring (Sherr et al. 1999). This suggests that a small portion of bacteria plays a significant role in material cycling. If the active bacterial fraction is assumed to be 20% in terms of PO_4 uptake, which coincides with the ratio of nucleoid-containing cells to total bacterial counts at the same site (Zweifel and Hagström 1995), the mean affinity constant would be similar to that of cyanobacteria. Yet the values are still ~5 times lower than the theoretical maximum (Fig. 7). However, we have no data of the active fraction of bacterial community, and, thus, no correction was not made for this (Fig. 4).

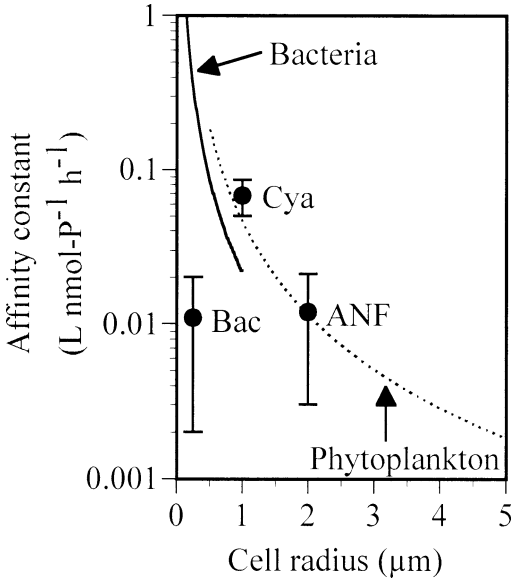

Fig. 7. Comparison of the mean estimated affinity constants (±SD, $n = 14$) of bacteria, cyanobacteria, and ANFs vs. the theoretical maximum of affinity constants by the diffusion model. The solid and dotted lines denote the theoretical maximum for bacteria and phytoplankton, respectively. The assumption for the diffusion model is that the diffusion constant for the substrate molecules is 10^{-5} cm^2 s^{-1}, cell density is 1.2 g cm^{-3}, dry weight is 50% of wet weight of cell, carbon weight is 50% of dry weight of cell, and the molar C : P ratio is 50 for bacteria and 106 for phytoplankton. See text for details.

P transfer rates in the food web—The incubation of filtrates from different pore-sized filters showed that the top-down control was significant, although predator-prey interactions were temporally variable. It appeared that virus concentrates stimulated the bacterial growth rate. SRP and TDP concentrations showed only a slight increase in virus concentrated water (data not shown). Limiting substrate(s) other than P might be enhanced during the filtration and concentration process.

In cold-chase experiments, we observed (1) a net increase of ^{32}P in the largest size fraction (>2 μm), (2) a net loss of ^{32}P in smaller fractions (0.2–0.6 and 0.6–2 μm), and (3) no significant difference in P release rates between in the <0.6

μm and the <0.6 μm + V filtrates. These results suggest that ^{32}P was transferred into a larger size fraction (i.e., higher trophic level) via predation and that viruses were not significant in P release. Hudson and Taylor (1996) reported that the release rate was enhanced with high concentrations of cold chase (>160 μmol L^{-1}) in Ranger Lake. Significant decreases of ^{32}P in the 0.2–0.6 and 0.6–2 μm fractions were detected in the <2 and 0.6 μm filtrates that included few or no predators (Fig. 6). In such cases, our cold chase (100 or 200 μmol L^{-1}) appeared to chase labels from osmotrophs.

P release rates of ≈ 0 to 0.5% of added ^{32}P h^{-1} detected in cold-chase experiments indicate that the turnover time of particulate P—that is, the microbial community—was at least 8.3 d. This is up to two orders of magnitude greater than that of orthophosphate (0.04–3.9 d) during the study period. The range of release rates (0.06–0.16 nmol P L^{-1} h^{-1}) of the microbial community was lower than those measured at Ranger and Mouse Lakes (0.5–6.6 nmol P L^{-1} h^{-1}; Hudson and Taylor 1996). However, in Villefranche Bay, the average dissolved phosphorus was 93% of total P (TDP + particulate P; range, 85%–98%), and the turnover time of orthophosphate was 0.67–5 h during the stratified period (Dolan et al. 1995; Thingstad et al. 1998; present study), which is quite different from those in the lakes where the average particulate P was 66% of total P (range, 43%–81%) and the turnover time was 0.02–0.83 h (Hudson et al. 1999, 2000). Even if the system is supposed to be P limited or deficient, the fundamental mechanism of P cycling may be different between freshwater and seawater.

P flow in the food web—Estimated concentrations of bioavailable free orthophosphate (1.3–2.3 nmol L^{-1}) are comparable to the <1 nmol L^{-1} level that was found at the same site (Dolan et al. 1995), in the brackish layer of a Norwegian fjord (Thingstad et al. 1993), and in P limited limnetic systems (Hudson et al. 2000). This is also comparable to the chemically measured dissolved inorganic phosphate (0.2–1 nmol L^{-1}) in the western north Atlantic Ocean (Wu et al. 2000). On the other hand, DOP (384–834 nmol L^{-1}) was two orders of magnitude greater than bioavailable free orthophosphate in the present study. Because orthophosphate uptake was dominated by APFs + cyanobacteria in three experiments, our flow diagram demonstrated that HNFs, which ingest ''winning competitors'' among osmotrophs, and their predators (small ciliates) are quantitatively important for P release. P release rates calculated from the flow diagram (0.14–0.29 nmol P L^{-1} h^{-1}) were slightly greater than those estimated from cold-chase experiments (0.06–0.16 nmol P L^{-1} h^{-1}).

The calculated turnover time of HPF-P (0.2–0.7 h) appears to be too short. This can be because of errors in biomass P estimation (see discussion above), the size fraction of bacterivores (here assumed <2 μm), and the high transfer efficiency from prey to predator (90%–96%). However, if we decrease the transfer efficiency from prey to predator, this increases not only the turnover time of predator P but also the P release rate. This then gives greater differences in the P release rate between P transfer experiments and P flow diagrams. We found that the bacterial biomass P was estimated to be 1.5–7 times greater for microscope-based than particulate P–based measurements. It has been reported that heterotrophic flagellates sized <5 μm are mainly bacterivores (Rassoulzadegan and Sheldon 1986). The overestimation of bacterial biomass and the underestimation of bacterivore biomass could result in such short turnover times of HPF-P. In future, it will be necessary to develop a P flow diagram that better describes predator-prey and virus-host interactions in the microbial food web and to improve the methods for measuring biomass P.

In summary, we found that the DOP concentration was much greater than SRP and particulate P during the study period and that the turnover time of orthophosphate was short in surface mixed water until the water column stratification was broken. This is consistent with the findings of previous studies (Thingstad and Rassoulzadegan 1995; Dolan et al. 1995). The fraction of orthophosphate uptake was greatly dominated by cyanobacteria. We revealed that estimated affinity constants of cyanobacteria and ANFs were almost at the maximum predicted by the diffusion model, whereas those of heterotrophic bacteria were much lower than the theoretical maximum. This suggests that cyanobacteria were the winning competitors for PO_4 uptake. In cold-chase experiments, although a net loss of ^{32}P was detected in different size fractions, P release from the microbial food web was relatively slow ($<0.5\%$ h^{-1}). In consequence, the turnover time of particulate P (<200 μm) was up to three orders of magnitude longer than that of orthophosphate in autumn in Villefranche Bay.

References

BRATBAK, G., AND T. F. THINGSTAD. 1985. Phytoplankton-bacteria interactions: An apparent paradox? Analysis of a model system with both competition and commensalism. Mar. Ecol. Prog. Ser. **25:** 23–30.

BUSTILLOS-GUZMÁN, J., H. CLAUSTRE, AND J.-C. MARTY. 1995. Specific phytoplankton signatures and their relationship to hydrographic conditions in the coastal northwestern Mediterranean Sea. Mar. Ecol. Prog. Ser. **124:** 247–258.

CARON, D. A., AND OTHERS. 1995. The contribution of microorganisms to particulate carbon and nitrogen in surface waters of the Sargasso Sea near Bermuda. Deep-Sea Res. **42:** 943–972.

CHISHOLM, S. W., R. J. OLSON, E. R. ZETTLER, R. GOERICKE, J. B. WATERBURY, AND N. A. WELSCHMEYER. 1988. A novel free-living prochlorophyte abundant in the oceanic euphotic zone. Nature **334:** 340–343.

DOLAN, J. R., T. F. THINGSTAD, AND F. RASSOULZADEGAN. 1995. Phosphate transfer between microbial size-fractions in Villefranche Bay (N. W. Mediterranean Sea), France in autumn 1992. Ophelia **41:** 71–85.

FAGERBAKKE, K. M., M. HELDAL, AND S. NORLAND. 1996. Content of carbon, nitrogen, oxygen, sulfur and phosphorus in native aquatic and cultured bacteria. Aquat. Microb. Ecol. **10:** 15–27.

HAGSTRÖM, Å., F. AZAM, A. ANDERSSON, J. WIKNER, AND F. RASSOULZADEGAN. 1988. Microbial loop in an oligotrophic pelagic marine ecosystem: Possible roles of cyanobacteria and nanoflagellates in the organic fluxes. Mar. Ecol. Prog. Ser. **49:** 171–178.

HEISSENBERGER, A., G. G. LEPPARD, AND G. J. HERNDL. 1996. Relationship between the intracellular integrity and the morphology of the capsular envelope in attached and free-living marine bacteria. Appl. Environ. Microbiol. **62:** 4521–4528.

HUDSON, J. J., AND W. D. TAYLOR. 1996. Measuring regeneration

of dissolved phosphorus in planktonic communities. Limnol. Oceanogr. **41:** 1560–1565.

———, ———, AND D. W. SCHINDLER. 1999. Planktonic nutrient regeneration and cycling efficiency in temperate lakes. Nature **400:** 659–661.

———, ———, AND ———. 2000. Phosphate concentrations in lakes. Nature **406:** 54–56.

JUMARS, P. A., J. W. DEMING, P. S. HILL, L. KARP-BOSS, P. K. YAGER, AND W. B. DADE. 1993. Physical constraints on marine osmotrophy in an optimal foraging context. Mar. Microb. Food Webs **7:** 121–159.

KOROLEFF, F. 1976. Determination of phosphorus, p. 125–131. *In* K. Grasshoff [ed.], Methods in seawater analysis. Verlag Chemie.

KROM, M. D., N. KRESS, S. BRENNER, AND L. I. GORDON. 1991. Phosphorus limitation of primary productivity in the eastern Mediterranean Sea. Limnol. Oceanogr. **36:** 424–432.

LEE, S., AND J. A. FUHRMAN. 1987. Relationships between biovolume and biomass of naturally derived marine bacterioplankton. Appl. Environ. Microbiol. **53:** 1298–1303.

MOUTIN, T., T. F. THINGSTAD, F. VAN WAMBEKE, D. MARIE, G. SLAWYK, P. RAIMBAULT, AND H. CLAUSTRE. 2002. Is the predominance of cyanobacteria *Synechococcus* related to competition for phosphate at nanomolar level? Limnol. Oceanogr. **47:** 1562–1567.

PENGERUD, B., E. F. SKJOLDAL, AND T. F. THINGSTAD. 1987. The reciprocal interaction between degradation of glucose and ecosystem structure. Studies in mixed chemostat cultures of marine bacteria, algae, and bacterivorous nanoflagellates. Mar. Ecol. Prog. Ser. **35:** 111–117.

PORTER, K. G., AND Y. S. FEIG. 1980. The use of DAPI for identifying and counting aquatic microflora. Limnol. Oceanogr. **25:** 943–948.

PUTT, M., AND D. K. STOECKER. 1989. An experimentally determined carbon: Volume ratio for marine ''oligotrichous'' ciliates from estuarine and coastal waters. Limnol. Oceanogr. **34:** 1097–1103.

RASSOULZADEGAN, F. 1979. Cycles annuels de la distribution de différentes catégories de particules du seston et essai d'identification des principales poussées phytoplanctoniques dans les eaux néritiques de Villefranche-sur-Mer. J. Exp. Mar. Biol. Ecol. **38:** 41–56.

———, AND R. W. SHELDON. 1986. Predator-prey interactions of nanozooplankton and bacteria in an oligotrophic marine environment. Limnol. Oceanogr. **31:** 1010–1021.

REDFIELD, A. C., B. H. KETCHUM, AND F. A. RICHARDS. 1963. The influence of organisms on the composition of sea water, p. 26–77. *In* M. N. Hill [ed.], The sea. Vol. 2. Interscience.

RIGLER, F. H. 1966. Radiobiological analysis of inorganic phosphorus in lakewater. Verh. Int. Ver. Limnol. **16:** 465–470.

SHERR, E. B., B. F. SHERR, AND C. T. SIGMON. 1999. Activity of marine bacteria under incubated and in situ conditions. Aquat. Microb. Ecol. **20:** 213–223.

SOKAL, R. R., AND F. J. ROHLF. 1995. Biometry, 3rd ed. W.H. Freeman.

SERVICE D'OBSERVATION EN MILIEU LITTORAL. 2000. Available at: http://www.obs-vlfr.fr/somlit/home.html.

SUTTLE, C. A., J. A. FUHRMAN, AND D. G. CAPONE. 1990. Rapid ammonium cycling and concentration-dependent partitioning of ammonium and phosphate: Implications for carbon transfer in planktonic communities. Limnol. Oceanogr. **35:** 424–433.

THINGSTAD, T. F., AND R. LIGNELL. 1997. Theoretical models for the control of bacterial growth rate, abundance, diversity and carbon demand. Aquat. Microb. Ecol. **13:** 19–27.

———, AND F. RASSOULZADEGAN. 1995. Nutrient limitations, microbial food webs, and ''biological C-pumps'': Suggested interactions in a P-limited Mediterranean. Mar. Ecol. Prog. Ser. **117:** 299–306.

———, AND ———. 1999. Conceptual models for the biogeochemical role of the photic zone microbial food web, with particular reference to the Mediterranean Sea. Prog. Oceanogr. **44:** 271–286.

———, E. F. SKJOLDAL, AND R. A. BOHNE. 1993. Phosphorus cycling and algal-bacterial competition in Sandsfjord, western Norway. Mar. Ecol. Prog. Ser. **99:** 239–259.

———, U. L. ZWEIFEL, AND F. RASSOULZADEGAN. 1998. P limitation of heterotrophic bacteria and phytoplankton in the northwest Mediterranean. Limnol. Oceanogr. **43:** 88–94.

VADSTEIN, O. A. 2000. Heterotrophic, planktonic bacteria and cycling of phosphorus—phosphorus requirements, competitive ability, and food web interactions. Adv. Microb. Ecol. **16:** 115–167.

———, AND Y. OLSEN. 1989. Chemical composition and phosphate uptake kinetics of limnetic bacterial communities cultured in chemostats under phosphorus limitation. Limnol. Oceanogr. **34:** 939–946.

VERITY, P. G., AND C. LANGDON. 1984. Relationships between lorica volume, carbon, nitrogen, and ATP content of tintinnids in Narragansett Bay. J. Plankton Res. **6:** 859–868.

WRIGHT, R. T., AND J. E. HOBBIE. 1966. Use of glucose and acetate by bacteria and algae in aquatic systems. Ecology **47:** 447–464.

WU, J., W. SUNDA, E. A. BOYLE, AND D. M. KARL. 2000. Phosphate depletion in the Western North Atlantic Ocean. Nature **289:** 759–762.

ZOHARY, T., AND R. D. ROBARTS. 1998. Experimental study of microbial P limitation in the eastern Mediterranean. Limnol. Oceanogr. **43:** 387–395.

ZWEIFEL, U. K., AND Å. HAGSTRÖM. 1995. Total counts of marine bacteria include a large fraction of non–nucleoid-containing bacteria (ghosts). Appl. Environ. Microbiol. **61:** 2180–2185.

———, B. NORRMAN, AND Å. HAGSTRÖM. 1993. Consumption of dissolved organic carbon by marine bacteria and demand for inorganic nutrients. Mar. Ecol. Prog. Ser. **101:** 23–32.

Received: 31 July 2002
Accepted: 10 January 2003
Amended: 28 January 2003